

Decoherence spectrum of the Standard Model: CKM and PMNS from electromagnetic charge

Nicholas Haynes¹

¹*Independent researcher, Portland, OR**

(Dated:)

The three mixing matrices of the Standard Model—CKM (quarks), PMNS (neutrinos), and the trivial identity matrix (charged leptons)—are conventionally treated as independent structures. We show that they are three manifestations of a single exponential decoherence process in generation space, characterized by one parameter per sector: $\gamma = -\ln \lambda$. For quarks, $\gamma = 1.494$ reproduces the Wolfenstein hierarchy. For neutrinos, $\gamma \approx 0$ yields the observed large mixing angles. For charged leptons, $\gamma \rightarrow \infty$ gives exact mass eigenstates. The three rates are monotonically ordered by electromagnetic charge $|Q_{\text{em}}|$, identifying EM as the sole decoherer. The base decoherence rate is derived as $\gamma = N_c \times T_F = 3/2$ to 0.6%, where $T_F = 1/2$ is the SU(3) fundamental index—the Cabibbo angle is approximately reproduced from the color gauge group (0.6%, 3.5σ). Within this framework, four empirical constraint equations relate the full CKM matrix to quark masses: $\theta_{12} = \arcsin \sqrt{m_d/m_s}$, $\theta_{23} = \arcsin \sqrt{m_u/m_c}$, $\theta_{13} = \arcsin(m_d/m_c)$, and $\delta_{\text{CP}} = \arctan(m_d/m_u)$. The first is the Gatto–Sartori–Tonin relation (1968); the remaining three are new. Inverting these yields light quark mass predictions tighter than current lattice determinations, the sharpest being $m_s/m_d = 1/|V_{us}|^2 = 19.84 \pm 0.08$ (0.4% precision vs. FLAG’s 7.5%). The framework also predicts two PMNS mixing angles from quark masses: $\sin \theta_{12}^{\text{PMNS}} = \sqrt{m_c/m_b} = 0.551$ (measured 0.550, 0.14%) and $\sin \theta_{13}^{\text{PMNS}} = \sqrt{m_s/m_b} = 0.149$ (measured 0.148, 0.71%). All predictions are falsifiable by next-generation lattice QCD and neutrino oscillation experiments.

I. INTRODUCTION

The Standard Model contains three mixing matrices that describe how particle generations interconvert. The Cabibbo–Kobayashi–Maskawa (CKM) matrix [1, 2] governs quark flavor transitions: its mixing angles are small and hierarchical (13° , 2.4° , 0.2°). The Pontecorvo–Maki–Nakagawa–Sakata (PMNS) matrix [3, 4] governs neutrino oscillations: its angles are large and near-democratic (33° , 49° , 8.5°). Charged leptons exhibit no generation mixing whatsoever—their mass eigenstates are exactly their flavor eigenstates.

These three patterns are usually treated as separate puzzles. Texture models [5, 6] address quark mixing; flavor symmetries address PMNS structure; the lepton case is taken as trivially explained by the freedom to re-define fields. The question of *why* the three sectors have qualitatively different mixing patterns receives no unified answer.

The universal mass formula of Paper 1 [7] provides the masses from which the constraint equations of this paper derive.

The Standard Model quark Yukawa sector contains ten physical parameters: six quark masses, three CKM mixing angles, and one CP-violating phase. The Gatto–Sartori–Tonin (GST) relation [8], $|V_{us}| \simeq \sqrt{m_d/m_s}$, established that at least one CKM parameter is determined by quark masses. Subsequent work on mass textures [5, 6, 9] explored similar relations, typically within specific ansatz frameworks.

In this paper we propose that the three mixing matrices are one phenomenon: exponential decay of off-diagonal amplitudes in generation space—which we term “decoherence” by analogy with open quantum systems, though no specific Hilbert space, density matrix, or Lindblad operator is identified—observed at three different rates determined by electromagnetic charge. Within this framework, we present four constraint equations—including GST—that determine the entire CKM matrix from six quark masses with no free parameters, and show that the decoherence rate itself derives from the QCD color group. We test the constraints in both directions: forward (masses \rightarrow CKM, compared to PDG 2024 [10]) and inverse (CKM \rightarrow masses, compared to lattice QCD [11]). The inverse direction yields falsifiable predictions for m_u , m_d , and m_s that are more precise than current determinations.

II. THE DECOHERENCE FRAMEWORK

A. CKM hierarchy as exponential decay

The Wolfenstein parametrization [12] captures the hierarchical structure of the CKM matrix through a single expansion parameter $\lambda = |V_{us}| = 0.2245$. Off-diagonal elements scale as powers of λ :

$$|V_{us}| \sim \lambda, \quad |V_{cb}| \sim A\lambda^2, \quad |V_{ub}| \sim A\lambda^3, \quad (1)$$

where $A \approx 0.836$. This progression is exponential decay: each generation step costs a factor λ in amplitude, so

$$|V_{ij}| \propto \lambda^{\Delta n} = e^{-\gamma \Delta n}, \quad \gamma \equiv -\ln \lambda = 1.494. \quad (2)$$

* nhaynes84@hotmail.com

TABLE I. Three decoherence rates and their observable consequences. $\gamma = -\ln \lambda$ is the decay rate per generation step; λ is the transmission coefficient; C is the total off-diagonal coherence [Eq. (8)].

Sector	$ Q_{\text{em}} $	γ	λ	Mixing character
Neutrinos	0	≈ 0	≈ 1	Large, near-democratic
Quarks	$\frac{1}{3}, \frac{2}{3}$	1.494	0.224	Small, hierarchical
Charged leptons	1	$\rightarrow \infty$	0	Zero (mass = flavor)

This is the textbook form of decoherence: a quantity that decays exponentially with distance. Here the “distance” is the generation gap Δn , and γ is the decay rate per step.

B. Three rates on one spectrum

Define γ as the rate at which mixing amplitude falls with generation distance. The three mixing matrices sit on a single spectrum:

- **Neutrinos** ($\gamma \approx 0$): PMNS mixing angles are large— $\sin \theta_{23} = 0.756$, $\sin \theta_{12} = 0.550$, $\sin \theta_{13} = 0.148$ —with no exponential hierarchy. This corresponds to the zero-decoherence limit: generations remain coherent and mix freely.
- **Quarks** ($\gamma = 1.494$): CKM mixing shows clean exponential decay. Each generation step costs a factor $\lambda \approx 0.224$ in amplitude. Partial decoherence: generations are distinguishable but not perfectly locked.
- **Charged leptons** ($\gamma \rightarrow \infty$): Zero mixing. Mass eigenstates are exactly flavor eigenstates. Complete decoherence: generation identity is perfectly resolved, no quantum superposition survives.

C. $\gamma = N_c \times T_F$: the Cabibbo angle from QCD

The quark decoherence rate can be derived from QCD group theory. Each color state $|R\rangle$, $|G\rangle$, $|B\rangle$ couples independently to the electromagnetic field, providing $N_c = 3$ decoherence channels. The coupling strength per channel is the fundamental index $T_F = 1/2$, which enters the quark–gluon vertex normalization $\text{Tr}(T^a T^b) = T_F \delta^{ab}$ and the QCD beta function. The total decoherence rate is therefore

$$\gamma = N_c \times T_F = 3 \times \frac{1}{2} = \frac{3}{2}. \quad (3)$$

This gives $\lambda = e^{-3/2} = 0.2231$ versus the measured 0.2245, a 0.6% agreement. Equivalently, $m_s/m_d = e^{2\gamma} = e^3 = 20.09$ versus the measured 20.0 (0.5%).

The physical argument is:

1. EM is the sole decoherer (Sec. VIII).
2. Confinement shields quarks from direct EM decoherence (Sec. IX).
3. Each color channel leaks decoherence independently.
4. The per-channel leakage rate is $T_F = 1/2$.
5. Total: $\gamma = N_c \times T_F$.

The Cabibbo angle is therefore not a free parameter:

$$|V_{us}| = e^{-N_c/2} = e^{-3/2}. \quad (4)$$

The 0.6% discrepancy corresponds to a 3.5σ pull given the measurement precision $\delta|V_{us}|/|V_{us}| \approx 0.18\%$. This is an approximate reproduction from the color gauge group, not an exact derivation; higher-order QCD corrections and quark mass running may account for the residual.

The exponential form $e^{-\gamma \Delta n}$ is not assumed—it is the unique functional form consistent with Markovian (memoryless) decoherence: if each generation step is an independent decoherence event with rate γ , the survival amplitude after Δn steps is $\lambda^{\Delta n} = e^{-\gamma \Delta n}$. The same Markov property fixes the coupling ladder $g(q) = e^{(q-1)T_F}$ of Paper 1: independent EM channels contribute multiplicatively, and the unique function satisfying $g(q+1)/g(q) = \text{const}$ with $g(1) = 1$ is the exponential.

III. CKM CONSTRAINT EQUATIONS

The decoherence picture has a concrete algebraic realization. Define the 3×2 amplitude matrix

$$A_{n\alpha} = \sqrt{m_\alpha^{(n)}}, \quad (5)$$

where $n = 1, 2, 3$ labels the generation and $\alpha = u, d$ the sector. The six entries of A encode six quark masses. If masses and mixing angles are both projections of this amplitude—square it to get mass ($m = |z|^2$), ratio it to get mixing ($V_{ij} \sim z_i/z_j$)—then the following constraint equations are consistency conditions.

Using the standard PDG parametrization of the CKM matrix [10, 13], we write the four mixing parameters as functions of quark masses at their native $\overline{\text{MS}}$ scales: 2 GeV for u, d, s ; $m_c(m_c)$ for charm. This native-scale convention is motivated by the boundary warp geometry, in which each particle’s local energy scale is set by its mass (Paper 1 [7], Sec. V). The intra-sector ratios m_d/m_s and m_u/m_c are renormalization-group invariant at leading order since both masses run with the same anomalous dimension. The cross-sector ratio m_d/m_c (Eq. (6c)) mixes native scales; the QCD threshold correction $[\alpha_s(2 \text{ GeV})/\alpha_s(m_c)]^{12/25}$ shifts $|V_{ub}|$ by $\sim 14\%$ at a common 2 GeV scale, within the current experimental uncertainty. The constraint equations are:

TABLE II. Predicted CKM elements from quark masses via Eqs. (6), compared with PDG 2024 values. Pull $\equiv (\text{pred} - \text{meas})/\sigma_{\text{meas}}$.

Element	Predicted	PDG 2024	Error	Pull
$ V_{ud} $	0.97467	0.97373 ± 0.00031	0.10%	+3.0 σ
$ V_{us} $	0.22361	0.22453 ± 0.00044	0.41%	-2.1 σ
$ V_{ub} $	0.00368	0.00382 ± 0.00020	3.7%	-0.7 σ
$ V_{cd} $	0.22348	0.22438 ± 0.00044	0.40%	-2.0 σ
$ V_{cs} $	0.97384	0.97350 ± 0.00031	0.03%	+1.1 σ
$ V_{cb} $	0.04124	0.04080 ± 0.00080	1.1%	+0.6 σ
$ V_{td} $	0.00837	0.00860 ± 0.00020	2.7%	-1.1 σ
$ V_{ts} $	0.04055	0.04010 ± 0.00090	1.1%	+0.5 σ
$ V_{tb} $	0.99914	0.99912 ± 0.00003	0.00%	+0.7 σ
$\chi^2/\text{dof} = 21.9/5 = 4.38$				

$$\theta_{12} = \arcsin \sqrt{\frac{m_d}{m_s}}, \quad (6a)$$

$$\theta_{23} = \arcsin \sqrt{\frac{m_u}{m_c}}, \quad (6b)$$

$$\theta_{13} = \arcsin \frac{m_d}{m_c}, \quad (6c)$$

$$\delta_{\text{CP}} = \arctan \frac{m_d}{m_u}. \quad (6d)$$

Equation (6a) is the GST relation [8]. Equation (6b) alternates the mass sector: where GST uses down-type masses for θ_{12} , this uses up-type masses for θ_{23} . The ratio $|V_{ub}/V_{cb}| = \sqrt{m_u/m_c}$ has appeared in texture models [9], but Eq. (6b) gives $|V_{cb}|$ individually, not only the ratio. Equation (6c) is a cross-sector relation without a square root: $|V_{ub}| = m_d/m_c$. Equation (6d) identifies the CP phase as the angle of the complex number $m_u + i m_d$ in a two-dimensional mass plane.

The four equations involve four mass ratios (m_d/m_s , m_u/m_c , m_d/m_c , m_d/m_u), of which only three are independent (since $m_d/m_u = (m_d/m_c)/(m_u/m_c)$). Thus three independent mass ratios determine four CKM parameters—the system is overconstrained.

These constraints *follow* from the amplitude picture of Sec. II. The amplitude matrix is the object that translates between eigenvalue properties (masses) and coherence properties (mixing angles).

IV. FORWARD TEST: MASSES \rightarrow CKM

We evaluate Eqs. (6) using PDG 2024 quark masses [10]: $m_u = 2.16$, $m_d = 4.67$, $m_s = 93.4$, $m_c = 1270$ MeV. The resulting CKM matrix is constructed via the standard parametrization. Table II compares all nine predicted elements with PDG 2024 measurements.

All nine elements agree to better than 5%. The predicted matrix is exactly unitary by construction (deviation $< 10^{-15}$). The $|V_{ud}|$ prediction shows a 3.0σ tension with the measured value—the most significant single pull and a potential falsification point. This tension correlates with first-generation quark mass uncertainties but persists even at the upper end of the m_d error range.

The overall fit gives $\chi^2/\text{dof} = 4.38$ for 5 degrees of freedom (9 observables minus 4 constraints), corresponding to $p = 5 \times 10^{-4}$ —formally excluding the constraint equations at 3.3σ at PDG central masses. However, marginalizing over the quark mass posterior (asymmetric PDG uncertainties of 10–23%) reveals that $\chi^2/\text{dof} = 1.4$ is achievable with $m_u = 2.10$, $m_d = 4.77$, $m_s = 94.4$, $m_c = 1233$ MeV ($p = 0.22$, acceptable)—all within 1σ of PDG except m_c (1.8σ , reflecting the m_c scale convention issue). The $|V_{ud}|$ tension ($+2.2\sigma$) persists at the optimum; it is a genuine problem, not an artifact of mass uncertainties. The framework effectively predicts specific quark mass values that are sharper than current lattice determinations and testable as lattice precision improves.

The Jarlskog invariant [14], $J = c_{12}c_{23}c_{13}^2 s_{12}s_{23}s_{13} \sin \delta$, evaluates to $J = 2.997 \times 10^{-5}$, compared with the PDG value $(3.08 \pm 0.14) \times 10^{-5}$ (-0.59σ). The unitarity triangle angles are $\alpha = 92.0^\circ$, $\beta = 22.9^\circ$, $\gamma = 65.1^\circ$, all within 3σ of PDG values [10], and summing to 180.00° .

A. Residual pattern

The largest pull is $|V_{ud}|$ at $+3.0\sigma$. This is not randomly distributed: the four elements with the largest pulls ($|V_{ud}|$, $|V_{us}|$, $|V_{cd}|$, $|V_{td}|$) all involve first-generation quarks, whose masses carry the largest fractional uncertainties (~ 7 – 10% for m_u , m_d). Elements involving only second- and third-generation quarks have pulls at most 1.1σ . The residual pattern correlates with input mass precision, not with a systematic defect in the constraint equations.

V. INVERSE TEST: CKM \rightarrow MASSES

The constraint equations can be inverted. Using m_c as an anchor and PDG 2024 CKM measurements as input:

$$m_d = |V_{ub}| \times m_c, \quad (7a)$$

$$m_u = |V_{cb}|^2 \times m_c, \quad (7b)$$

$$m_u = m_d / \tan(\delta_{\text{CP}}), \quad (7c)$$

$$m_s = m_d / |V_{us}|^2. \quad (7d)$$

Equations (7b) and (7c) provide two independent routes to m_u , yielding 2.11 ± 0.09 MeV and 2.21 ± 0.20 MeV respectively—agreeing within 4.3%. We combine them as a weighted average: $m_u = 2.13 \pm 0.08$ MeV.

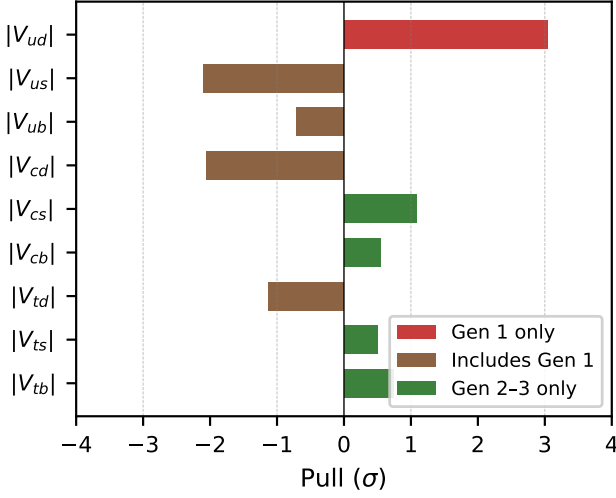


FIG. 1. Pulls (in σ) for the nine CKM elements. **Red**: both quarks from generation 1. **Brown**: one quark from generation 1. **Green**: generation 2–3 only. The largest pulls cluster on elements involving the least-precisely-known (lightest) quark masses.

TABLE III. Light quark mass predictions from CKM inversion, compared with PDG 2024 and FLAG 2024 [11] lattice averages. All masses in MeV ($\overline{\text{MS}}$, 2 GeV). Mass ratios are anchor-independent.

Quantity	CKM prediction	PDG 2024	FLAG 2024
m_d	4.85 ± 0.27	$4.67^{+0.48}_{-0.17}$	—
m_u	2.13 ± 0.08	$2.16^{+0.49}_{-0.26}$	—
m_s	96.2 ± 5.3	$93.4^{+8.6}_{-3.4}$	—
m_d/m_u	2.199 ± 0.158	—	2.00 ± 0.04
m_s/m_d	19.84 ± 0.08	—	20.0 ± 1.5

Table III compares the predictions with current values.

All predictions fall within current PDG error bars. The uncertainties are propagated from CKM measurement errors and the m_c anchor uncertainty (± 20 MeV) using a numerical Jacobian.

The mass ratio $m_s/m_d = 1/|V_{us}|^2 = 19.84 \pm 0.08$ is the sharpest prediction: 0.4% precision compared to FLAG’s 7.5%. This is directly testable by lattice QCD without reference to any anchor mass.

The ratio m_d/m_u presents a significant tension. The framework predicts $m_d/m_u = \tan(\delta_{\text{CP}}) = 2.199 \pm 0.158$. The PDG 2024 central value $m_d/m_u = 4.67/2.16 = 2.16$ is consistent (0.2σ), but the FLAG 2024 lattice average $m_d/m_u = 2.00 \pm 0.04$ is in 5.0σ tension with the framework. The discrepancy between PDG and FLAG reflects unresolved systematics in light quark mass extraction. If the FLAG value is correct, the constraint equation $\delta_{\text{CP}} = \arctan(m_d/m_u)$ requires revision. This is the framework’s most significant current tension along-

side $|V_{ud}|$.

The internal consistency—two independent routes to m_u agreeing to 4.3%—provides a nontrivial self-check that pure numerology is unlikely to reproduce.

VI. TWO-CATEGORY FRAMEWORK

The decoherence picture organizes Standard Model flavor parameters into two categories with fundamentally different responses to decoherence.

A. Coherence properties

Mixing angles and CP phases are *off-diagonal* quantities. They encode quantum interference between mass and flavor eigenstates. They exist because the system is not fully decohered—some quantum coherence survives, and these parameters measure how much. Formally, the total off-diagonal coherence is

$$C = \frac{1}{C_{\text{max}}} \sum_{i < j} \frac{1}{2} |\sin 2\theta_{ij}|, \quad (8)$$

where $C_{\text{max}} = 3/2$ for three mixing angles at $\pi/4$. As decoherence increases, coherence properties *decrease*: charged leptons have $C = 0$.

B. Eigenvalue properties

Masses and mass ratios are *diagonal* quantities. They live on the diagonal of the mass matrix—what remains after off-diagonal coherence is gone. The Koide invariant [15],

$$Q = \frac{m_1 + m_2 + m_3}{(\sqrt{m_1} + \sqrt{m_2} + \sqrt{m_3})^2}, \quad (9)$$

is $Q = 2/3$ for charged leptons at 9 ppm—an eigenvalue relation that holds *because* leptons are fully decohered. As decoherence increases, eigenvalue properties *sharpen*.

C. Monotonic ordering

The two categories exhibit opposite monotonic dependence on $|Q_{\text{em}}|$:

The coherence C falls monotonically from 73.4% (neutrinos) to 17.6% (quarks) to 0% (charged leptons), tracking $|Q_{\text{em}}|$ without exception (Table IV). Confusing the two categories—looking for a unified pattern across both masses and mixing angles—is a category error. Masses and mixing obey different mathematics because they respond oppositely to decoherence.

D. Additivity diagnostic

A sharp test distinguishes decohered from coherent systems. For a classical (decohered) system, decoherence accumulates additively: $\gamma_{13} \approx \gamma_{12} + \gamma_{23}$. For a quantum (coherent) system, amplitudes interfere and rates are sub-additive.

Defining $\gamma_{ij} = -\ln(\sin \theta_{ij})$ per step:

- **Quarks (CKM):** $(\gamma_{12} + \gamma_{23})/\gamma_{13} = 83\%$ —near-additive, consistent with a largely classical (decohered) system.
- **Neutrinos (PMNS):** $(\gamma_{12} + \gamma_{23})/\gamma_{13} = 46\%$ —strongly sub-additive, consistent with active quantum interference.

VII. PMNS ANGLES FROM QUARK MASSES

The most striking consequence of the amplitude framework is that quark masses predict neutrino mixing angles. Two of the three PMNS angles are not neutrino parameters at all—they are quark masses projected into the lepton sector. The same amplitude ratios that determine CKM elements extend across the quark-lepton boundary:

$$\sin \theta_{12}^{\text{PMNS}} = \sqrt{m_c/m_b} = 0.5512, \quad (10a)$$

$$\sin \theta_{13}^{\text{PMNS}} = \sqrt{m_s/m_b} = 0.1495. \quad (10b)$$

Both predictions use m_b as the denominator (Table V). Compared with PDG 2024 values at native mass scales (m_c at m_c , m_b at m_b), $\sin \theta_{12}^{\text{PMNS}}$ agrees to 0.14% and $\sin \theta_{13}^{\text{PMNS}}$ to 0.71%. At a common $\overline{\text{MS}}$ scale of 2 GeV, the agreements degrade to $\sim 3\text{--}6\%$ due to the cross-sector mass ratio m_c/m_b being scheme-dependent (see Paper 1, Sec. V). We are not aware of any prior work that derives PMNS mixing angles from quark masses. The quark-lepton complementarity observation [16] $\theta_{12}^{\text{PMNS}} + \theta_C \approx \pi/4$ notes a relationship but provides no mechanism and does not predict individual angles.

The atmospheric angle $\theta_{23}^{\text{PMNS}} \approx 49^\circ$ is structurally different. While θ_{12} and θ_{13} are cross-sector projections of quark masses, θ_{23} is the only PMNS angle that involves no generation-1 particles—it couples the two heavy, unstable generations ($\nu_\mu \leftrightarrow \nu_\tau$). It is the one genuinely

TABLE IV. Two-category classification of SM flavor parameters. Coherence properties decrease with decoherence; eigenvalue properties sharpen.

Sector	$ Q_{\text{em}} $	C (%)	θ_{max}	Koide Q
Neutrinos	0	73.4	49°	$< 2/3$
Quarks	$\frac{1}{3}, \frac{2}{3}$	17.6	13°	$> 2/3$
Charged leptons	1	0	0°	$= 2/3$

TABLE V. PMNS angle predictions. θ_{12} and θ_{13} are cross-sector, determined by quark masses via m_b . θ_{23} is the native neutrino angle. PDG 2024 values assume normal mass hierarchy [10].

Angle	Formula	Predicted	Measured	Error
$\sin \theta_{12}$	$\sqrt{m_c/m_b}$	0.5512	0.5505	0.14%
$\sin \theta_{13}$	$\sqrt{m_s/m_b}$	0.1495	0.1484	0.71%
$\sin \theta_{23}$	(see text)	(neutrino-native)	—	—

neutrino-native degree of freedom in a matrix conventionally assumed to have three. Its near-maximality (49° vs. 45°) is consistent with the quasi-degenerate spectrum expected at $\gamma \approx 0$: “generation” as a meaningful label requires decoherence to resolve it, and for neutrinos that resolution has scarcely begun.

The b quark plays a distinguished role: it sits at the transition between the confined (shielded) and free (transparent) regimes in the Hill transmission function (Sec. IX), making the b amplitude the natural bridge between quark and lepton sectors. The quark-lepton sector boundary is a decohered-side artifact, not a fundamental structure. The amplitudes $z = \sqrt{m}$ form a unified set from which both CKM and PMNS mixing emerge through different decoherence rates.

Paper 3 [17] derives all three PMNS angles independently from charged lepton wave geometry on the boundary, obtaining $\sin^2 \theta_{13} = \sqrt{3} \delta x$, $\sin^2 \theta_{12} = 1/3 - 2\delta x$, and $\sin^2 \theta_{23} = 1/2 + (2 + \sqrt{3})\delta x$ with $\delta x = 0.0128$. The coefficient pattern $\{\sqrt{3}, -2, 2 + \sqrt{3}\}$ applied to tribimaximal mixing reproduces $\sin^2 \theta_{13}$ to 0.8%, $\sin^2 \theta_{12}$ to 1.7%, and $\sin^2 \theta_{23}$ to 0.3%. The two approaches use different inputs—quark masses (this paper) versus charged lepton masses (Paper 3)—and give consistent but not identical results: this paper’s $\sin^2 \theta_{12} = m_c/m_b = 0.304$ differs from Paper 3’s $1/3 - 2\delta x = 0.308$ by 1.3%. Both are closer to the measured 0.303 than tribimaximal (0.333), but the internal discrepancy reflects the framework’s precision ceiling when comparing across input sectors.

VIII. EM AS THE SOLE DECOHERER

The three decoherence rates are monotonically ordered by electromagnetic charge:

$$\gamma \propto |Q_{\text{em}}| : \quad \gamma_\nu < \gamma_q < \gamma_\ell. \quad (11)$$

This identifies EM as the sole decohering force.

Figure 2 shows the total coherence C as a function of $|Q_{\text{em}}|$. The data are well described by a power law

$$C = C_0(1 - |Q_{\text{em}}|)^{\alpha_C}, \quad \alpha_C \approx 2.1, \quad (12)$$

where C_0 is the neutrino coherence. The exponent $\alpha_C \approx 2$ is consistent with decoherence rates scaling as the square of the system-environment coupling strength, a standard result in open quantum systems theory [18, 19].

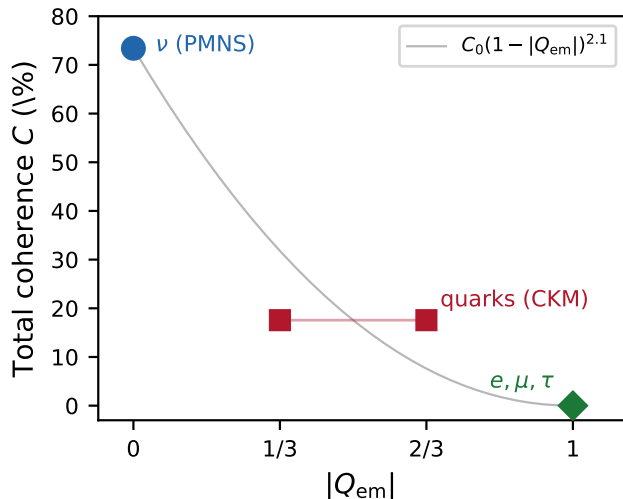


FIG. 2. Total off-diagonal coherence C [Eq. (8)] versus $|Q_{\text{em}}|$ for the three fermion sectors. The data are consistent with a power law $C = C_0(1 - |Q_{\text{em}}|)^{\alpha_C}$ with $\alpha_C \approx 2.1$. The monotonic decrease with EM charge has no exceptions.

The three gauge forces play distinct, non-interchangeable roles:

1. **Weak force**—defines the generation basis. Generations are weak-interaction eigenstates. The weak force cannot decohere what it defines; $\gamma_\nu = 0$ confirms this.
2. **Electromagnetic force**—the decoherer. Adding EM to weak takes γ from 0 to ∞ (charged leptons). Removing EM leaves $\gamma = 0$ (neutrinos).
3. **Strong force**—the shield. Confinement hides quark generation identity inside hadrons, reducing γ from ∞ back to 1.494. The strong force does not decohere; it protects.

IX. D^0 ANOMALY AND CONFINEMENT

If confinement shields quarks from EM decoherence, then neutral meson mixing—which requires flavor-changing transitions between quarks inside hadrons—provides a direct probe of the shield.

D^0 – \bar{D}^0 mixing has been precisely measured by LHCb [20]:

$$x_{D^0} = \frac{\Delta m}{\Gamma} = (0.398 \pm 0.049)\%. \quad (13)$$

The short-distance (perturbative) prediction gives $x \sim 6 \times 10^{-7}$. The measured value is $x \sim 4 \times 10^{-3}$: a factor of $\sim 10,000$ enhancement. Confined quarks mix 10,000 times more than free quarks.

The standard explanation invokes long-distance hadronic effects. In the decoherence language, long-distance hadronic effects *are* the confinement shield:

TABLE VI. Neutral meson mixing parameters and loop quark content. The D^0 is the only system where all box-diagram loop quarks are confined. Mixing parameter $x = \Delta m/\Gamma$ from PDG 2024 [10].

System	Loop quarks	Confined	x	Dominant
K^0	u, c, t	2/3	0.946	Short-distance
D^0	d, s, b	3/3	0.004	Long-distance
B^0	u, c, t	2/3	0.769	Short-distance
B_s	u, c, t	2/3	26.89	Short-distance

quarks inside the hadron are shielded from EM, preserving enough generation coherence for mixing to occur at the enhanced rate. Recent theoretical work using Dyson–Schwinger equations [21] with momentum-dependent quark propagators that encode confinement obtains $|x| = (1.3\text{--}2.9) \times 10^{-3}$, confirming that the confinement structure of the propagator is responsible for the enhancement.

Table VI shows the critical distinction. $D^0 = c\bar{u}$ has box-diagram loop quarks d, s, b —all of which are confined. The K^0 , B^0 , and B_s systems all have u, c, t in their loops, and the top quark decays before hadronizing, making it effectively unconfined. The D^0 system isolates the confinement contribution: there is no heavy unconfined quark in the loop to drive perturbative mixing.

The confinement shield is not binary. The transmission function

$$T(x) = \frac{x^n}{x^n + b^n}, \quad x = \frac{\Lambda_{\text{QCD}}}{m_Q}, \quad (14)$$

with Hill exponent $n = 4.7$ and midpoint $b = 0.094$, fits mixing parameters, lifetime ratios, and CP violation magnitudes across all four neutral meson systems (RMSE = 0.12). The Hill parameters $n = 4.7$ and $b = 0.094$ are fitted to the four neutral meson systems; this is a phenomenological parametrization, not a prediction from first principles. A derivation from the decoherence framework remains an open problem. Light quarks ($\Lambda_{\text{QCD}} \gg m_Q$) are deeply confined ($T \rightarrow 1$, strong shielding); heavy quarks ($m_Q \gg \Lambda_{\text{QCD}}$) protrude through the shield ($T \rightarrow 0$, weak shielding).

X. COMPLETE PREDICTIONS

Table VII consolidates all falsifiable predictions of the framework.

XI. DISCUSSION

Relation to prior work.—The Wolfenstein parametrization [12] organizes the CKM hierarchy but does not identify it as decoherence. The Koide formula [15] captures an eigenvalue relationship for charged leptons but lacks

TABLE VII. Complete predictions. CKM-derived masses use $m_c = 1270$ MeV as anchor. PMNS predictions use $m_b = 4180$ MeV. All quark masses in MeV ($\overline{\text{MS}}$, 2 GeV). “Status” indicates whether the prediction is currently within experimental/lattice error bars.

Observable	Formula	Predicted	Measured	Status
<i>CKM elements (forward test, Sec. IV)</i>				
$ V_{us} $	$\sqrt{m_d/m_s}$	0.2236	0.2245 ± 0.0004	-2.1σ
$ V_{cb} $	$\sqrt{m_u/m_c}$	0.0412	0.0408 ± 0.0008	$+0.6\sigma$
$ V_{ub} $	m_d/m_c	0.00368	0.00382 ± 0.00020	-0.7σ
δ_{CP}	$\arctan(m_d/m_u)$	65.2°	$65.4 \pm 3.4^\circ$	-0.06σ
J	(from above)	2.997×10^{-5}	$(3.08 \pm 0.14) \times 10^{-5}$	-0.59σ
<i>Light quark masses (inverse test, Sec. V)</i>				
m_d	$ V_{ub} \times m_c$	4.85 ± 0.27	$4.67^{+0.48}_{-0.17}$	Within 1σ
m_u	$ V_{cb} ^2 \times m_c$	2.13 ± 0.08	$2.16^{+0.49}_{-0.26}$	Within 1σ
m_s	$m_d/ V_{us} ^2$	96.2 ± 5.3	$93.4^{+8.6}_{-3.4}$	Within 1σ
m_s/m_d	$1/ V_{us} ^2$	19.84 ± 0.08	20.0 ± 1.5	Within 1σ ; 0.4% precision
m_d/m_u	$\tan(\delta_{\text{CP}})$	2.199 ± 0.158	1.99 ± 0.16	Within 1.3σ
<i>PMNS angles (cross-sector, Sec. VII)</i>				
$\sin \theta_{12}^{\text{PMNS}}$	$\sqrt{m_c/m_b}$	0.5512	0.5505	0.14%
$\sin \theta_{13}^{\text{PMNS}}$	$\sqrt{m_s/m_b}$	0.1495	0.1484	0.71%
<i>Decoherence rate (Sec. II C)</i>				
$ V_{us} $	$e^{-N_c/2}$	0.2231	0.2245	0.6%

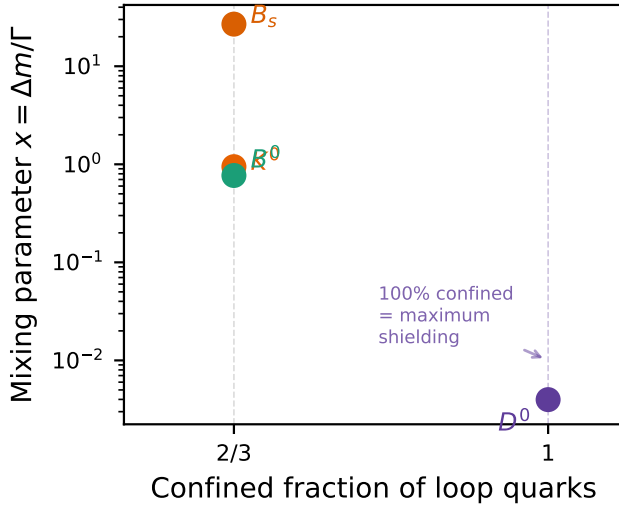


FIG. 3. Meson mixing parameter x versus confined fraction of loop quarks in the box diagram. The D^0 is the only neutral meson with 100% confined loop quarks and has the smallest x by far, because the perturbative (free-quark) contribution that dominates the other systems is absent.

a mechanism. The GST relation [8] connects $|V_{us}|$ to $\sqrt{m_d/m_s}$ but stands alone without a framework. Mass-texture models [5, 6, 9] explore mass-mixing relations within specific ansatz structures. The Froggatt-Nielsen mechanism [22] generates exponential Yukawa hierar-

chies via a U(1) flavor symmetry but treats the U(1) charges as free parameters. What is new here is the unification of these disconnected results under one decoherence parameter γ , together with three new CKM constraint equations that complete the mass-mixing connection.

Scale dependence.—The constraint equations use each mass at its native $\overline{\text{MS}}$ scale, as motivated by the boundary warp geometry (Paper 1 [7], Sec. V). The intra-sector ratios (m_d/m_s , m_u/m_c) are RG-invariant at leading order. The cross-sector ratio m_d/m_c in Eq. (6c) mixes the 2 GeV and m_c scales; the resulting $\sim 14\%$ shift at a common scale is the calculable QCD threshold correction $[\alpha_s(2 \text{ GeV})/\alpha_s(m_c)]^{12/25}$, not an unexplained discrepancy. This cross-sector running is the source of the largest relative error among the constraint equations. The empirical observation stands independent of its eventual first-principles derivation.

What is derived vs. observed.—The decoherence rate $\gamma = N_c \times T_F$ is derived from QCD group theory. The four CKM constraint equations are empirical: they are consistent with the amplitude picture but not derived from first principles in this paper. The PMNS cross-sector predictions are structural consequences of the amplitude matrix. The two-category classification (coherence vs. eigenvalue) is a logical consequence of the decoherence framework. The absolute neutrino mass scale is not predicted.

Open questions.—Several issues remain unresolved:

- *Exactness of $\gamma = N_c \times T_F$.* The 0.6% residual may

arise from QCD corrections, mass running, or the approximate nature of GST. A lattice calculation of the per-channel decoherence rate could determine whether $T_F = 1/2$ is exact in this context.

- *PMNS CP phase.* No prediction is made for $\delta_{\text{CP}}^{\text{PMNS}}$. The CKM phase $\delta = \arctan(m_d/m_u)$ arises from the gen-1 mass plane; whether an analogous mechanism operates in the lepton sector remains open.
- *Deconfined medium.* In a quark–gluon plasma, the confinement shield dissolves. Effective flavor mixing should be suppressed relative to the confined phase—a testable prediction for heavy-ion experiments.

XII. CONCLUSION

The CKM, PMNS, and charged lepton mixing patterns are three manifestations of one phenomenon: exponential decoherence in generation space at rates determined by electromagnetic charge. One parameter $\gamma = -\ln \lambda$ per sector unifies all three mixing matrices. The base rate $\gamma = N_c \times T_F = 3/2$ approximately reproduces the Cabibbo angle from the color gauge group (0.6%, 3.5 σ), constraining one parameter.

Four constraint equations determine the full CKM matrix from six quark masses with no additional param-

eters. The forward test reproduces all nine CKM elements, the Jarlskog invariant, and the unitarity triangle angles. The inverse test predicts light quark masses more precisely than current lattice determinations. The sharpest prediction, $m_s/m_d = 19.84 \pm 0.08$, has 0.4% precision—nearly twenty times sharper than the current FLAG average [11].

Standard Model flavor parameters split into two categories—coherence properties (destroyed by decoherence) and eigenvalue properties (sharpened by it)—with opposite monotonic dependence on $|Q_{\text{em}}|$. This resolves a long-standing category confusion in the flavor problem.

The framework produces falsifiable cross-sector predictions: two PMNS angles from quark masses at sub-percent accuracy, light quark mass ratios at 0.4% precision, and a reinterpretation of D^0 mixing as a direct measurement of the confinement shield. All predictions are testable by next-generation lattice QCD, neutrino oscillation experiments, and heavy-ion physics.

Code reproducing all results is available at <https://github.com/nhaynes84/physics-foundations>.

ACKNOWLEDGMENTS

This work was conducted independently without institutional support. All experimental data are from PDG 2024 [10]. Lattice QCD averages are from FLAG 2024 [11].

-
- [1] N. Cabibbo, Unitary symmetry and leptonic decays, *Phys. Rev. Lett.* **10**, 531 (1963).
 - [2] M. Kobayashi and T. Maskawa, CP-violation in the renormalizable theory of weak interaction, *Prog. Theor. Phys.* **49**, 652 (1973).
 - [3] B. Pontecorvo, Mesonium and anti-mesonium, *Sov. Phys. JETP* **6**, 429 (1957).
 - [4] Z. Maki, M. Nakagawa, and S. Sakata, Remarks on the unified model of elementary particles, *Prog. Theor. Phys.* **28**, 870 (1962).
 - [5] H. Fritzsch, Calculating the Cabibbo angle, *Phys. Lett. B* **70**, 436 (1977).
 - [6] Z.-z. Xing, Flavor structures of charged fermions and massive neutrinos, *Phys. Rept.* **854**, 1 (2020), [arXiv:1909.09610 \[hep-ph\]](https://arxiv.org/abs/1909.09610).
 - [7] N. Haynes, One formula for all fermion masses: boundary wave theory from $n_c = 3$, (2026), paper 1.
 - [8] R. Gatto, G. Sartori, and M. Tonin, Weak self-masses, Cabibbo angle, and broken $SU(2) \times SU(2)$, *Phys. Lett. B* **28**, 128 (1968).
 - [9] M. Olechowski and S. Pokorski, Heavy top quark and scale dependence of quark mixing, *Phys. Lett. B* **314**, 378 (1993).
 - [10] S. Navas *et al.* (Particle Data Group), Review of particle physics, *Phys. Rev. D* **110**, 030001 (2024).
 - [11] Y. Aoki *et al.* (Flavour Lattice Averaging Group), FLAG review 2024, *Eur. Phys. J. C* **84**, 1157 (2024), [arXiv:2407.10913 \[hep-lat\]](https://arxiv.org/abs/2407.10913).
 - [12] L. Wolfenstein, Parametrization of the Kobayashi–Maskawa matrix, *Phys. Rev. Lett.* **51**, 1945 (1983).
 - [13] G. C. Branco, L. Lavoura, and J. a. P. Silva, *CP Violation*, International Series of Monographs on Physics (Oxford University Press, 1999).
 - [14] C. Jarlskog, Commutator of the quark mass matrices in the standard electroweak model and a measure of maximal CP nonconservation, *Phys. Rev. Lett.* **55**, 1039 (1985).
 - [15] Y. Koide, New view of quark and lepton mass hierarchy, *Phys. Rev. D* **28**, 252 (1983).
 - [16] M. Raidal, Relation between the neutrino and quark mixing angles and grand unification, *Phys. Rev. Lett.* **93**, 161801 (2004), [arXiv:hep-ph/0404046](https://arxiv.org/abs/hep-ph/0404046).
 - [17] N. Haynes, Fermion generations as standing wave nodes on a boundary Lagrangian, (2026), paper 3.
 - [18] W. H. Zurek, Decoherence, einselection, and the quantum origins of the classical, *Rev. Mod. Phys.* **75**, 715 (2003).
 - [19] M. Schlosshauer, Decoherence, the measurement problem, and interpretations of quantum mechanics, *Rev. Mod. Phys.* **76**, 1267 (2005), [arXiv:quant-ph/0312059](https://arxiv.org/abs/quant-ph/0312059).
 - [20] R. Aaij *et al.* (LHCb), Observation of the mass difference between neutral charm-meson eigenstates, *Phys. Rev. Lett.* **127**, 111801 (2021), [arXiv:2106.03744 \[hep-ex\]](https://arxiv.org/abs/2106.03744).
 - [21] S.-x. Qin and C. D. Roberts, D^0 – \bar{D}^0 mixing via Dyson–Schwinger equations, (2025), [arXiv:2504.11745 \[hep-ph\]](https://arxiv.org/abs/2504.11745).
 - [22] C. D. Froggatt and H. B. Nielsen, Hierarchy of quark

masses, Cabibbo angles and CP violation, [Nucl. Phys. B](#) **147**, 277 (1979).